ACS OMEGA

Open Access

http://pubs.acs.org/journal/acsodf

Article

Identifying Potential Autophagy Modulators in Panch Phoron Spices (P5S): An In Silico approach

Sana Parveen, Shoeb Ikhlas, Tabrez Faruqui, Adria Hasan, Aisha Khatoon, Mohd Saeed, Ali G. Alkhathami, Samra Siddiqui, Shahab Uddin, and Snober S. Mir*

Cite This: *ACS Omega* 2025, 10, 871−884

Read Online

ACCESS | Metrics & More | Article Recommendations | Supporting Information

ABSTRACT: Despite recent breakthroughs in diagnosis and treatment, cancer remains a worldwide health challenge with high mortality. Autophagy plays a major role in the progression and development. Starving cancer cells obtain nutrients through the upregulation of autophagy. Several compounds derived from natural sources, including animals, plants, and microorganisms, have been identified as potential novel anticancer drugs. Spices play an important role in human health and possess many medicinal properties. Our study aimed to identify potential autophagy modulators from panch phoron spices (P5S) through in silico approaches. Herein, we report a structure-based virtual screening of compounds isolated from P5S (i.e., cumin, fenugreek, fennel, black mustard, and black cumin) against the molecular targets of autophagy. Using various computational tools, we attempted to identify potential modulators of autophagy. Among all the screening results (such as binding energy, hydrogen bonding, drug-likeness, bioactivity, ADME properties, and toxicity), P5S, stigmasterol, and tigogenin showed the best drug-like properties and binding affinity toward the selected targets of autophagy. Furthermore, the stability of both complexes was evaluated by performing a 100 ns molecular dynamics simulation (MDS) using Schrodinger's Desmond Module. Our results provide insight into the efficacy of P5S components against cancer. Therefore, targeting autophagy using these molecules may be an effective and potential drug candidate for cancer treatment. In conclusion, stigmasterol and tigogenin may act as potential candidates for anticancer drugs by targeting autophagy.

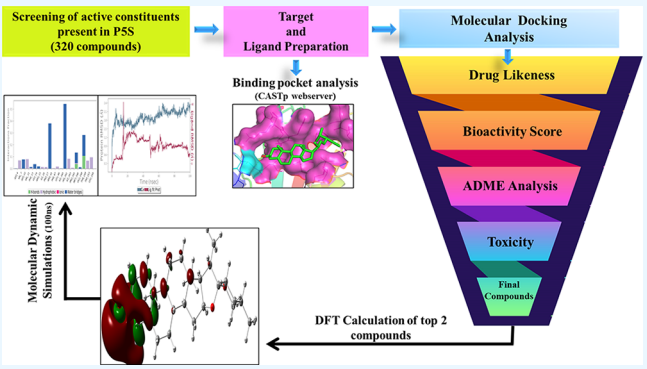

1. INTRODUCTION

Autophagy is a conserved catabolic process of protein and organelle quality control, in which bilayered vesicles enclose intracellular cytoplasmic macromolecules, damaged organelles, aggregated proteins, or pathogens, which are then transported to the lysosome for degradation by lysosomal hydrolases.[1,2] Autophagy is regulated by ATG genes (autophagy-related genes)[3] and helps in cancer cell survival but may also promote cell death. Cell death is generally associated with apoptosis.[4,5] However, both autophagy and apoptosis are essential for organismal homeostasis; hence, crosstalk occurs between the two, and this mechanism may be implicated in cancer.[6]

Cancer accounts for the second highest mortality rate worldwide, after cardiovascular diseases.[7] Chemotherapy and radiotherapy are first-line treatments for cancer. However, these anticancer approaches have various drawbacks such as drug resistance and off-target cytotoxicity.[8] Thus, compounds isolated from plants can be examined for anticancer activity. Natural plant-based compounds may reduce off-target cytotoxicity and help overcome drug resistance.[9]

Herbs and spices play an important role in the day-to-day life of humankind as flavoring agents in foods, beverages, and pharmaceuticals, as well as in perfumes and cosmetics.[10] A spice is the dried part of a plant, such as the bark, root, seed, fruit, or flower, used in small quantities for flavor, color, or as a preservative.[11] A mixture of five spices, Panch phoron comprising *Brassica nigra* (black mustard), *Trigonella foenum-graecum* Linn (fenugreek), *Foeniculum vulgare* (fennel), *Nigella sativa* (black cumin), and *Cuminum cyminum* (cumin),[12] was found to have antidiabetic, antioxidant, antimicrobial, anti-tumorigenic, anti-inflammatory, cardioprotective, and gastro-protective activities.[13] The anticancer potential of these spices is particularly noteworthy, as they contain various phytochemicals that have shown promising results in cancer prevention and treatment. Several studies have demonstrated the anticancer effects of spices on various types of cancer, including leukemia, myeloma, and carcinomas associated

Received: August 28, 2024
Revised: December 14, 2024
Accepted: December 24, 2024
Published: January 3, 2025

with the digestive tract.[14] For instance, black cumin (thymoquinone) and fennel (anethole) have been established as potential cancer-preventive agents.[15] The mechanisms by which these spices mediate anticancer effects are becoming increasingly evident, with many of them acting as potent antioxidants and anti-inflammatory agents, still more studies are required to explore other possible mechanisms.[16,17] The use of these natural products as medicinally active compounds represents a sustainable and green approach to healthcare, offering potential alternatives to synthetic drugs with fewer side effects.[16]

Thus, in this study, we examined the interaction of the active compounds of Panch phoron spices (P5S) with autophagy and the apoptotic markers ATG5 (autophagy protein 5), LC3 (microtubule-associated protein 1A/1B-light chain 3), and CASPASE-3. ATG5 is a marker gene for autophagy that is involved in the extension of the phagophore isolation membrane. LC3 is also a key regulator of autophagy, initiating autophagosome biogenesis after membrane conjugation through interactions with ATG7 and other autophagic effectors.[18,19] CASPASE-3 is a critical effector caspase that serves as a pivotal regulator in the balance between apoptosis and autophagy. Its activation is a hallmark of apoptosis, yet it also plays a crucial role in modulating autophagic processes.[20,21] Studies have shown that CASPASE-3 can cleave autophagy-related proteins, such as BECLIN-1 and ATG5, thereby inhibiting autophagic processes and promoting apoptosis.[22,23]

In this study, a total of 320 compounds were screened from various literature sources, of which 224 were docked through molecular docking. This study aimed to identify the potential interaction between apoptosis and autophagy markers, which may contribute to the chemoprotective potential of spices. The expected outcome of this study may help us to obtain better insights into the treatment of cancer by modulating autophagy.

2. METHODOLOGY

2.1. Phytoconstituent Screening. Preliminary screening of phytoconstituents is a critical step in elucidating their bioactive roles, which may facilitate the discovery and development of novel drugs. In this study, we conducted a comprehensive literature review to identify the phytoconstituents present in P5S utilizing databases such as Scopus, Google Scholar, and PubMed. The literature survey revealed approximately 320 bioactive compounds associated with P5S. Through a systematic analysis of the relevant literature, we specifically identified around 224 compounds, which were subsequently employed for molecular docking screening.

Furthermore, 5-FU was used as a positive control in this study. 5-FU functions as an antimetabolite, mimicking the structure of pyrimidines, which allows it to interfere with DNA and RNA synthesis. This mechanism is crucial for inducing cytotoxicity in rapidly dividing cancer cells. The drug inhibits thymidylate synthase, leading to the depletion of thymidine triphosphate (dTTP), which is essential for DNA replication.[24] Studies indicate that 5-FU can activate apoptotic pathways, leading to cell death through mechanisms involving caspases and the modulation of autophagy.[25−27] The unique mechanism of action of 5-FU can induce apoptosis and modulation of autophagy, and extensive clinical validation makes it a superior option compared to other natural and synthetic drugs as a positive control in our study. Its established role in cancer therapy provides a reliable benchmark against which new treatments can be compared.

2.2. Ligand and Target Preparation. The three-dimensional structures of the 224 P5S-derived compounds and positive control (5-FU) were obtained from the PubChem database (https://pubchem.ncbi.nlm.nih.gov/). The 2D structures of P5S-derived compounds and the positive control were generated using ChemDraw Ultra 7.0). The 3D structures of the main therapeutic targets of autophagy and apoptosis used in this study were ATG5, LC3, and CASPASE-3 (PDB IDs:4TQ1, 1UGM, and IRE1, respectively), available from the Protein Data Bank RCSB-PDB (https://www.rcsb.org/) in PDB format.[28] Energy minimization of the targets was performed using Swiss PDB Viewer 4.0.

2.3. Binding Site Identification. The Computed Atlas of Surface Topography of Proteins (CASTp) Web server (http://sts.bioe.uic.edu/castp/) was used to identify superficial and volumetric areas. The CASTp is a well-known indicator of potential binding sites. The specific binding sites were authenticated by metaPocket 2.0 (http://projects.biotec.tu-dresden.de/metapocket/) and the COACH-D (https://yanglab.nankai.edu.cn/COACH-D/) web server.

2.4. Structure-Based Molecular Interaction. Molecular docking is a virtual simulation technique that is widely used in in silico interaction studies between ligands and targets.[29] AutoDock 1.5.6 package was used to perform molecular docking to identify a potent autophagy modulator. It is a free, automated software developed by Molecular Graphics Lab, Scripps Research Institute (http://autodock.scripps.edu/). Essential hydrogen atoms, charges, and solvation parameters were added by using different AutoDock tools. The docking parameters were defined as coordinates of the center of the binding site at 126 × 126 ×126, 82 ×102 ×100, and 126 × 126 × 126 Å for ATG5, LC3, and CASPASE-3, respectively. Post docking, the 3D structure of the protein−ligand complex was visualized using Discovery Studio Visualizer 4.0. & Biovia Discovery Studio Visualizer.[30] The docking results were further validated using two additional docking software viz. CBDock[31] and DockThor software.[32]

2.5. Molinspiration Cheminformatics. Chemical structures and SMILES notations of the compounds were obtained from the PubChem database (https://pubchem.ncbi.nlm.nih.gov/). SMILES notations of active compounds are then fed into online software Molinspiration Cheminformatics to calculate different molecular physicochemical properties (Table 4) and to predict bioactivity scores for drug targets including enzymes and nuclear receptors, kinase inhibitors, GPCR ligands, and ion channel modulators. We have predicted the physicochemical properties with Lipinski's rule of five.[33]

2.6. PreADMET Properties Analysis. ADME property analysis of drug-like molecules is an important aspect to be considered during the drug development process. Multiple good drug candidates are unable to pass clinical trials because of their worse ADME profile.[34] Pre-ADMET software predicted the ADMET properties of the selected panch phoron-derived compounds.[35] Toxicity analysis was performed through online Data Warrior software.[36] Toxicity parameters, such as Tumorigenesis, Irritant, Reproductive Effect, and Mutagenicity, were evaluated. Toxicity is an important parameter to be evaluated in drug designing as it helps determine the toxic dose in animal model studies and lessens the number of animal model studies.[37]

https://doi.org/10.1021/acsomega.4c07924
ACS Omega 2025, 10, 871−884

2.7. In Silico Anticancer Sensitivity Prediction. With the help of the PaccMann Web server, we checked the anticancer sensitivity of selected compounds. It is a novel approach for the prediction of anticancer compound sensitivity through multimodal attention-based neural networks (https://ibm.biz/paccmann-aas). This model system ingests a compound's SMILES and the gene expression profile of a cancer cell and predicts an IC_{50} sensitivity value. With the help of this web server, we can predict the IC_{50} value of any drug-like-molecule.[38]

2.8. Density Functional Theory (DFT) Calculations. Calculation of the electron density surrounding the ligand molecule is important for establishing a stable bond between a target protein and a ligand molecule. In this study, Becke's three-parameter Lee−Yang−Parr hybrid functional (B3LYP) was chosen for the density functional theory calculations. All calculations were performed using the Gaussian 09 suite to generate the highest occupied molecular orbital (HUMO) and lowest unoccupied molecular orbital (LUMO) models of the selected molecules.[39−41]

2.9. Molecular Dynamics Simulations. Desmond (Schrödinger suite) was used to perform molecular dynamics simulations to elucidate the effectiveness of the selected compounds. The Protein Preparation Wizard Tool was used to prepare protein−ligand complexes.[42,43] The solvent model in an orthorhombic box was selected with 20 × 20 × 20 Å periodic boundary conditions as the transferable intermolecular interaction potential three points (TIP3P). The OPLS3e force field settings were employed and counterions (Na^+ or Cl^-) were applied.[44] An *NPT* ensemble with a pressure of 1 atm and a temperature of 300 K was used during the simulations. To stimulate the physiological parameters, 0.15 M NaCl was added. At different time intervals, the root-mean-square fluctuation (RMSF), root-mean-square deviation (RMSD), and protein−ligand interactions were recorded. The final production run was conducted for 100 ns. After the completion of simulations, the simulation interaction diagram was used for the analysis of the MD simulation trajectory using RMSD, RMSF, hydrogen bond analysis, and radius of gyration (R_g).

3. RESULTS

3.1. Molecular Docking Interaction of Screened P5S-Derived Active Compounds. Molecular docking was performed to evaluate the binding potential of all 224 P5S-derived compounds, and the positive control, 5-FU (5-FU, a well-known anticancer drug, was used as a positive control in the present study). The docking results showed that among all of the studied compounds, some had good interactions with the target molecules. After docking interactions of 224 compounds, top hit compounds in every panch phoron spice were selected for further studies. Details of all selected compounds are given in Table 1 and the chemical structure of these compounds are represented in Supplementary Figure 1.

The best binding affinity and inhibition constant of compounds of each spice with ATG5, LC3, and CASPASE-3, when docked for 100 runs, are listed below, along with the number of hydrogen bonds, interacting amino acids, and interacting amino acids with intermolecular H-bond (Table 2). Among all the interactions between the selected compounds, we found that stigmasterol and tigogenin showed the best interaction with the highest binding energy.

Table 1. Selected Top Hit Compounds in Every Spice of Panch Phoron with the Standard Drug 5-Fluorouracil

s. no.	spices	top hit compounds	Pubchem CID	molecular formula
1	control	5-fluorouracil (5-FU)	3385	$C_4H_3FN_2O_2$
2	cumin (*Cuminum cyminum*)	safranal	61041	$C_{10}H_{14}O$
3	fenugreek (*Trigonella foenum-graecum* Linn)	tigogenin	99516	$C_{27}H_{44}O_3$
4	fennel (*Foeniculum vulgare*)	*trans-p*-mentha-2,8-dienol	91753981	$C_{10}H_{16}O$
5	black mustard (*Brassica nigra*)	ascorbic acid	54670067	$C_6H_8O_6$
6	black cumin (*Nigella sativa*)	stigmasterol	5280794	$C_{29}H_{48}O$

Supplementary Figures 2−4 shows representative images of all 5-selected compounds with 5-FU which shows the best docking pose of ATG5, LC3, and CASPASE-3. Therefore, we analyzed the top-2 hit compounds (stigmasterol and tigogenin) binding pockets using the CASTp web server. It is evident from Table 2 in terms of binding energy (BE) and inhibition constant (IC) that stigmasterol and tigogenin displayed the best interaction with ATG5 (BE = −8.63, IC = 0.47056 μM and BE = −8.26, IC = 0.87837 μM respectively). In stigmasterol-ATG5 complex 1 hydrogen bond and Tyr36, Leu37, Leu38, Pro40, Leu47, Val48, Asp50, Lys51, Lys118, and Gln158 amino acid residues are involved. In tigogenin-ATG5 complex 1 hydrogen bond and Lys^5, Leu^8, Asp^{163}, Trp^{166}, Ala^{167}, Arg^{170}, Met^{173}, Glu^{256}, His^{257}, Phe^{162} amino acid residues are involved (Figure 1).

The molecular interaction with LC3 stigmasterol and tigogenin again shows the best interaction among all (BE = −8.35, IC = 0.75183 μM and BE = −7.90, IC = 1.62 μM, respectively). In stigmasterol-LC3 complex 2 hydrogen bond and Leu^{82}, Val^{83}, His^{86}, Ser^{87}, Met^{88}, Val^{89}, Ser^{90}, Thr^{93}, Glu^{97}, Val^{98}, Glu^{100}, Ser^{101}, and Glu^{102} amino acid residues are involved. In tigogenin-LC3 complex 1 hydrogen bond and Ile^{64}, Arg^{68}, Ala^{75}, Phe^{79}, Phe^{80}, Leu^{81}, Ser^{87}, Met^{88}, Val^{91}, and Glu^{117} amino acid residues are involved (Figure 2).

Further, the molecular interaction with LC3 stigmasterol and tigogenin again shows the best interaction among all top hit compounds (BE = −9.08, IC = 0.22262 μM and BE = −7.98, IC = 1.42 μM respectively). In stigmasterol-CASPASE-3 complex 2 hydrogen bond and Arg68, Leu^{90}, Thr^{92}, Pro^{93}, Gly^{94}, Arg^{95}, Ala^{96}, Ile^{98}, Ala^{100}, Val^{103}, Met^{104}, Gln^{107}, Lys^{173}, Ile^{174}, Asp^{177}, Tyr^{178}, Phe^{181} amino acid residues are involved. In tigogenin-CASPASE-3 complex 0 hydrogen bond and Arg^{68}, Ala^{96}, Ile^{98}, Ala^{100}, Val^{103}, Gln^{107}, Ser^{170}, Lys^{173}, Ile^{174}, Asp^{177}, Tyr^{178} amino acid residues are involved (Figure 3).

Docking calculations previously studied with Autodock were compared with new calculations carried out with CBDock and DockThor servers. Supplementary Tables 1 and 2 represent the best results obtained by molecular docking protocols with CBDock and DockThor. The compounds used in the screening process were ranked based on the binding energy, and the results were compared to the top 5 molecules that have the least binding energy in kcal/mol. The best binding complexes are ATG5- Stigmasterol (AutoDock binding energy = −8.63 kcal/mol, CB-Dock= −6.9 kcal/mol, and DockThor = −7.340 kcal/mol), ATG5-Tigogenin (AutoDock binding energy = −8.26 kcal/mol, CB-Dock= −6.2 kcal/mol, and

https://doi.org/10.1021/acsomega.4c07924
ACS Omega 2025, 10, 871−884

Table 2. Molecular Docking Analysis Predicted that Stigmasterol and Tigogenin Strongly Interact with All Selected Autophagy and Apoptotic Markers

active compounds	target proteins	binding energy (BE) (kcal/mol)	inhibition constant (IC) (μM)	interacting amino acid residues	no. of H bonds	hydrophobic interactions
5-FU	ATG-5	−4.70	356.86	Val,[7] Leu,[8] Arg,[9] Val,[11] Trp,[12] Phe[162], Phe[165], Trp[166], Asn[169], Glu[256], His[257], Leu[258], Ser[259], Tyr[260], Pro[261]	2	LEU A:8
						SER A:259
	LC3	−4.67	377.11	Gln[116],Tyr38, Gly,[40] Glu,[41] Lys,[42] Gln,[43] Ala[114], Ser[115]	4	LYS A:42
						GLN A:43
						GLU A:41
						GLN A:116
	CAS-3	−3.90	1390	Glu,[17] Asp,[18] Ser,[21] Ile,[69] Asn,[70] Tyr[106], Glu[110] , Arg[71] ,Asn[70]	3	ASP A: 18
						SER A:21
						TYR A:106
safranal	ATG-5	−7.20	5.27	Leu,[8] Val,[11] Trp,[12] Val,[42] Phe[165], Trp[166], Asn[169], Met[173], Glu[256], His[257], Leu[258], Ser[259]	1	ASN A:169
	LC3	− 6.12	32.50	Val,[20] Ile,[23] Arg,[24] His,[27] Pro,[28] Lys,[30] Ile,[31] Pro,[32] Tyr[99]	1	ARG A:24
	CAS-3	−4.96	233.22	Ala,[20] Lys,[23] Phe,[24] Leu,[27] Gln,[32] Gln,[35] Glu,[36] Asp[141], Ile[144]	1	GLN A:32
tigogenin	ATG-5	−8.26	0.87837	Lys,[5] Leu,[8] Asp[163], Trp[166], Ala[167], Arg[170], Met[173], Glu[256], His[257] ,Phe[162]	1	LYS A: 5
	LC3	−7.90	1.62	Ile,[64] Arg,[68] Ala[75], Phe[79], Phe[80], Leu[81], Ser[87], Met[88], Val[91], Glu[117]	1	MET A:88
	CAS-3	−7.98	1.42	Arg,[68] Ala[96], Ile[98], Ala[100], Val[103], Gln[107], Ser[170], Lys[173], Ile[174], Asp[177], Tyr[178]	0	
trans-p-mentha-2,8-dienol	ATG-5	−6.83	9.81	Val,[7] Leu,[8] Val,[11] Trp,[12] Phe[165], Trp[166], Asn[169], Met[173], Glu[256], His[257], Ser[259], Tyr[260], Pro[261], Asn[263]	0	
	LC3	−6.02	38.68	Met,[60] Val[83], His[86], Ser[87], Met[88], Val[89], Ser[90], Thr[93], Val[98], Ser[101], Glu[102]	2	SER A:90
						VAL A:89
	CAS-3	−5.16	166.11	Tyr[8], Gly,[11] Glu,[12] Leu,[14] Lys,[39] Asp,[40] Ala,[41] Leu[42]	2	GLY A:11
						ALA A:41
ascorbic acid	ATG-5	−6.42	19.64	Val,[7] Leu,[8] Arg,[9] Val,[11] Trp,[12] Phe[165], Trp[166], Asn[169], Met[173], His[241], His[257], Leu[258], Ser[259], Tyr[260], Pro[261], Asp[262], Asn[263] , Phe[162]	4	ASN A:169
						TYR A:260
						SER A: 259
						LEU A:8
	LC3	−5.57	82.10	Lys,[5] Thr[6], Phe,[7] Arg,[10] Ile,[35] Glu,[36] Arg,[37] Val,[46] Leu,[47] Lys,[49] Thr[50], Tyr[113]	5	ILE A:35
						THR A:50
						GLU A:36
						ARG A:37
						LEU A:47
	CAS-3	−4.64	394.18	Tyr[8], Gly,[11] Glu,[12] Leu,[14] Asp,[40] Ala,[41] Leu[42] , Leu[19]	5	LEU A:42
						ALA A:41
						GLY A:11
						LEU A:14
						GLU A:12
stigmasterol	ATG-5	−8.63	0.47056	Tyr[36], Leu,[37] Leu,[38] Pro,[40] Leu,[47] Val,[48] Asp,[50] Lys,[51] Lys[118], Gln[158]	1	LYS A:118
	LC3	−8.35	0.75183	Leu[82], Val[83], His[86], Ser[87], Met[88], Val[89], Ser[90], Thr[93], Glu[97], Val[98], Glu[100], Ser[101], Glu[102]	2	VAL A:83
						HIS A:86
	CAS-3	−9.08	0.22262	Arg68, Leu[90], Thr[92], Pro[93], Gly[94], Arg[95], Ala[96], Ile[98], Ala[100], Val103, Met[104], Gln[107], Lys[173], Ile[174], Asp[177], Tyr[178], Phe[181]	2	GLY A:94
						THR A:92

DockThor = −7.846 kcal/mol), and LC3- Stigmasterol (AutoDock binding energy = −8.35 kcal/mol, CB-Dock= −7.1 kcal/mol, and DockThor = −8.155 kcal/mol), LC3-Tigogenin (AutoDock binding energy = −7.90 kcal/mol, CB-Dock= −6.7 kcal/mol, and DockThor = −7.356 kcal/mol) and CASPASE-3- Stigmasterol (AutoDock binding energy = −9.08 kcal/mol, CB-Dock= −7.9 kcal/mol, and DockThor = −8.654 kcal/mol), CASPASE-3-Tigogenin (AutoDock binding energy = −7.98 kcal/mol, CB-Dock= −8.6 kcal/mol, and DockThor = −7.545 kcal/mol), respectively. The compounds were further screened for drug-likeness and toxicity parameters.

3.2. Drug Likeness and Physicochemical Parameters of Selected Compounds. With the help of molinspiration cheminformatics, drug-likeliness properties and molecular descriptors of compounds have been analyzed.[45] To ensure optimal bioavailability, an orally active medication candidate should not have more than one infraction of Lipinski's criteria.[46] The physicochemical properties of the selected compounds, such as partition coefficient (log *P*), hydrogen bond donors and acceptors, rotatable bonds, number of atoms, molecular weight, topological polar surface area (TPSA), and violations of Lipinski's rule of five, were calculated to evaluate

https://doi.org/10.1021/acsomega.4c07924
ACS Omega 2025, 10, 871−884

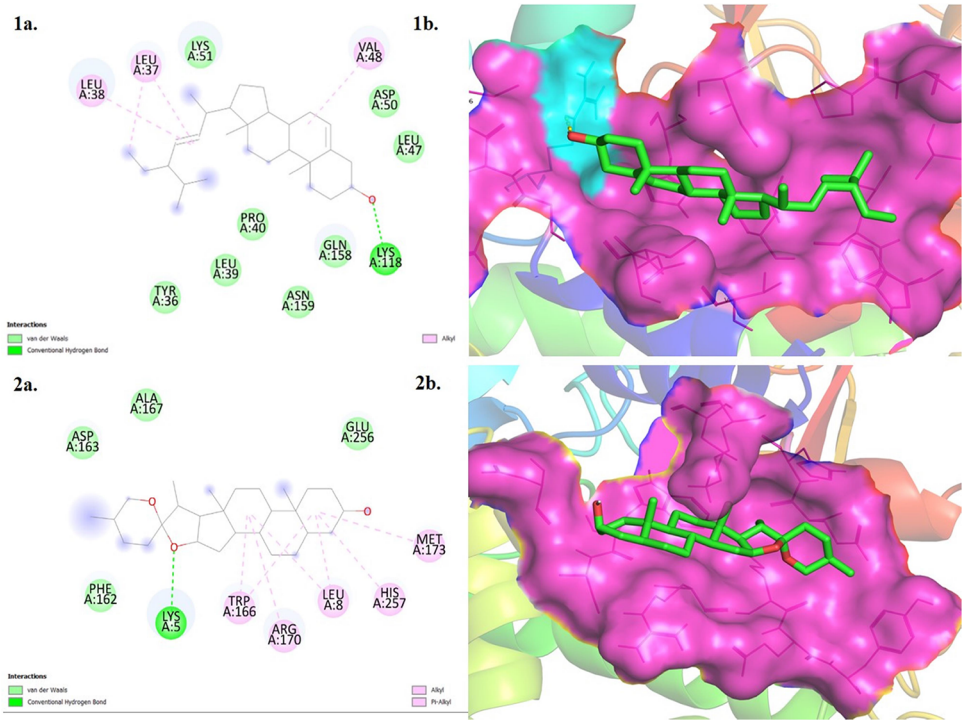

Figure 1. Representative images of the best docking pose of the (1a) ATG-5-stigmasterol complex (1b). The binding pocket at the ATG-5 domain is shown in the ATG5-stigmasterol complex and (2a) ATG-5-tigogenin complex (2b). The binding pocket at the ATG-5 domain is shown in the ATG5-tigogenin complex.

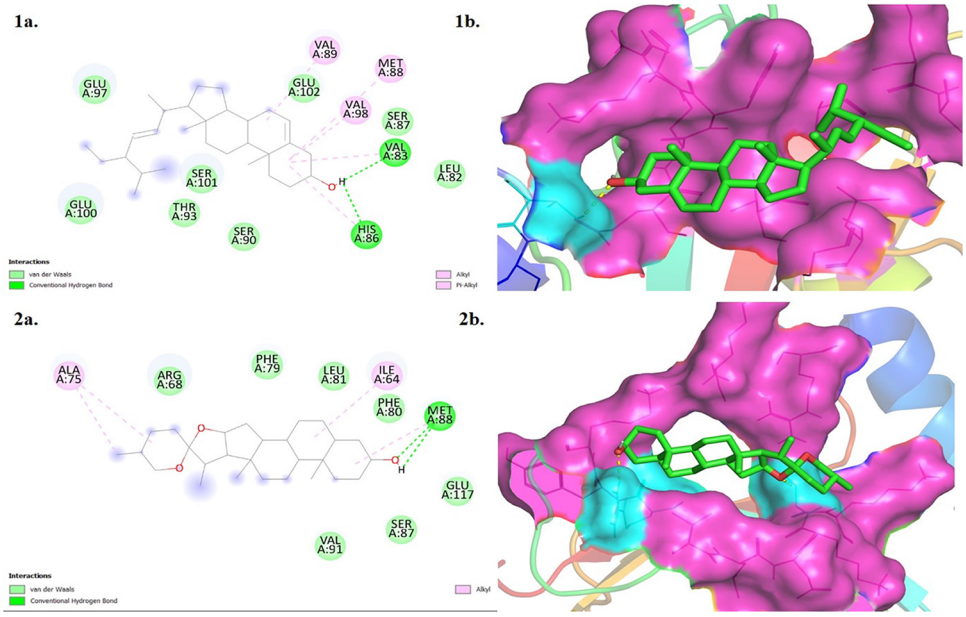

Figure 2. Representative images of the best docking pose of the (1a) LC3-stigmasterol complex (1b). The binding pocket at the LC3 domain is shown in the LC3-stigmasterol complex LC3-tigogenin complex and (2a) LC3-tigogenin complex (2b). The binding pocket at the LC3 domain is shown in the LC3-tigogenin complex.

the drug-likeness of the selected compounds (Table 3). The absorption percentage (% Ab) was also calculated by using the formula:

$$\%\text{Absorbance} = 109 - [0.345 \times \text{TPSA}]$$

These properties were calculated based on Lipinski's rule of five, which states that any compound considered the drug should have a partition coefficient less than 5, polar surface area within 140 Å, H bond acceptors less than 10, H bond donors less than 5, and molecular weight within 500 Da.[47] Among all compounds, tigogenin and stigmasterol were violated by one. Therefore, according to Table 3, none of the selected compounds exhibited more than one violation.

3.3. Bioactivity Score of Selected Compounds. With the help of molinspiration cheminformatics, we also checked molecular properties and bioactivity scores of selected

https://doi.org/10.1021/acsomega.4c07924
ACS Omega 2025, 10, 871−884

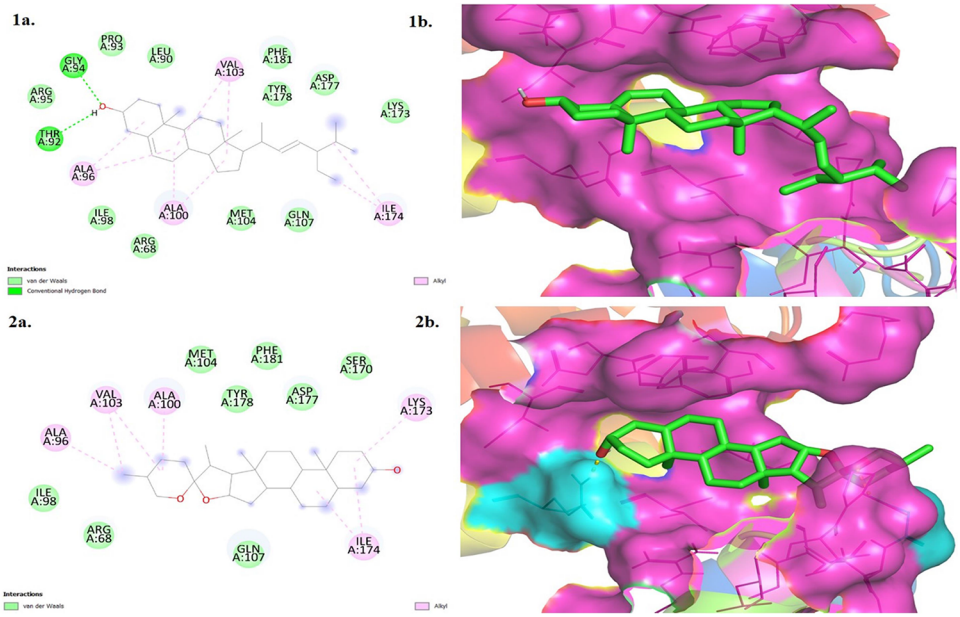

Figure 3. Representative images of the best docking pose of the (1a) CASPASE-3-stigmasterol complex (1b). The binding pocket at the CASPASE-3 domain is shown in the CASPASE-3-stigmasterol complex and (2a) CASPASE-3-tigogenin complex (2b). The binding pocket at the CASPASE-3 domain is shown in the CASPASE-3-tigogenin complex.

Table 3. Physicochemical Property Prediction of the Selected Panch Phoron-Derived Compounds Obtained from Molinspiration Cheminformatics

active compounds	% of absorption	topological polar surface area	molecular weight	miLog*P*	hydrogen bond donors (nOHNH)	hydrogen bond acceptors (nON)	number of rotatable bonds	Lipinski's violation
rules		<140	<500	≤5	<5	<10	≤10	≤1
5-FU	86.32%	65.72	130.08	−0.59	2	4	0	0
safranal	103%	17.07	150.22	2.95	0	1	1	0
tigogenin	95.6%	38.70	416.65	6.12	1	3	0	1
trans-p-mentha-2,8-dienol	102%	20.23	152.24	3.21	1	1	1	0
ascorbic acid	72%	107.22	176.12	−1.40	4	6	2	0
stigmasterol	102%	20.23	412.70	7.87	1	1	5	1

Table 4. Bioactivity Score of the Selected Panch Phoron-Derived Compounds Obtained from Molinspiration Cheminformatics[a]

compounds name	GPCR ligand	ion channel modulator	kinase inhibitor	nuclear receptor ligand	protease inhibitor	enzyme inhibitor
5-Fu	−2.60	−1.95	−2.62	−3.04	−3.15	−1.56
safranal	−0.99	−0.22	−1.24	−0.05	−0.94	0.07
tigogenin	0.13	0.15	−0.41	0.50	0.11	0.59
trans-p-mentha-2,8-dienol	−0.93	−0.39	−1.64	−0.66	−1.06	−0.18
ascorbic acid	−0.53	−0.24	−1.09	−1.01	−0.81	0.20
stigmasterol	0.12	−0.08	−0.48	0.74	−0.02	0.53

[a]Bioactivity; >Zero high probability, −0.50 to 0.00 moderate activity, and ← 0.50 inactive.

compounds and positive control. Molinspiration cheminformatics calculates the bioactivity score of selected compounds for G-protein coupled receptor (GPCR) ligands, ion channel modulators, kinase inhibitors, nuclear receptor ligands, protease inhibitors, and enzyme inhibitor targets. A compound having a bioactivity score greater than zero shows a high probability while a value of −0.50 to 0.00 shows moderate activity and if the score value is less than −0.50 considered to be inactive.[33,48] The bioactivity score data obtained showed that out of all selected compounds, stigmasterol and tigogenin show good GPCR ligand affinity. Obtained data indicate that stigmasterol has a better bioactivity score (Table 4).

3.4. Pre-ADMET Properties of Selected Compounds.

The ADMET properties of drugs play an important role in drug development. Compounds with unfavorable absorption, distribution, metabolism, and elimination have been identified as major causes of drug development failure. Among all the compounds, ascorbic acid showed a moderately absorbed human intestinal absorption value; safranal and ascorbic acid showed medium absorption in blood-brain barrier penetration and weak binding with plasma proteins. All compounds except ascorbic acid showed medium permeability in Caco-2 cells (Table 5).

https://doi.org/10.1021/acsomega.4c07924
ACS Omega 2025, 10, 871−884

Table 5. ADME Properties of the Selected Panch Phoron-Derived Compounds Obtained from the PreADMET Server[a]

	ADME properties					
compounds name	human intestine absorption (HIA)	blood brain barrier (BBB)	plasma protein binding	Caco2 cell permeability	GI absorption	skin permeability (log Kp)
5-FU	M	M	W	M	H	−7.73 cm/s
safranal	H	M	W	M	H	−5.70 cm/s
tigogenin	H	H	H	M	H	−4.23 cm/s
trans-p-mentha-2,8-dienol	H	H	H	M	H	−4.96 cm/s
ascorbic acid	M	M	W	W	H	−8.54 cm/s
stigmasterol	H	H	H	M	W	−2.74 cm/s

[a]W - Weak, M - Medium, and H - High.

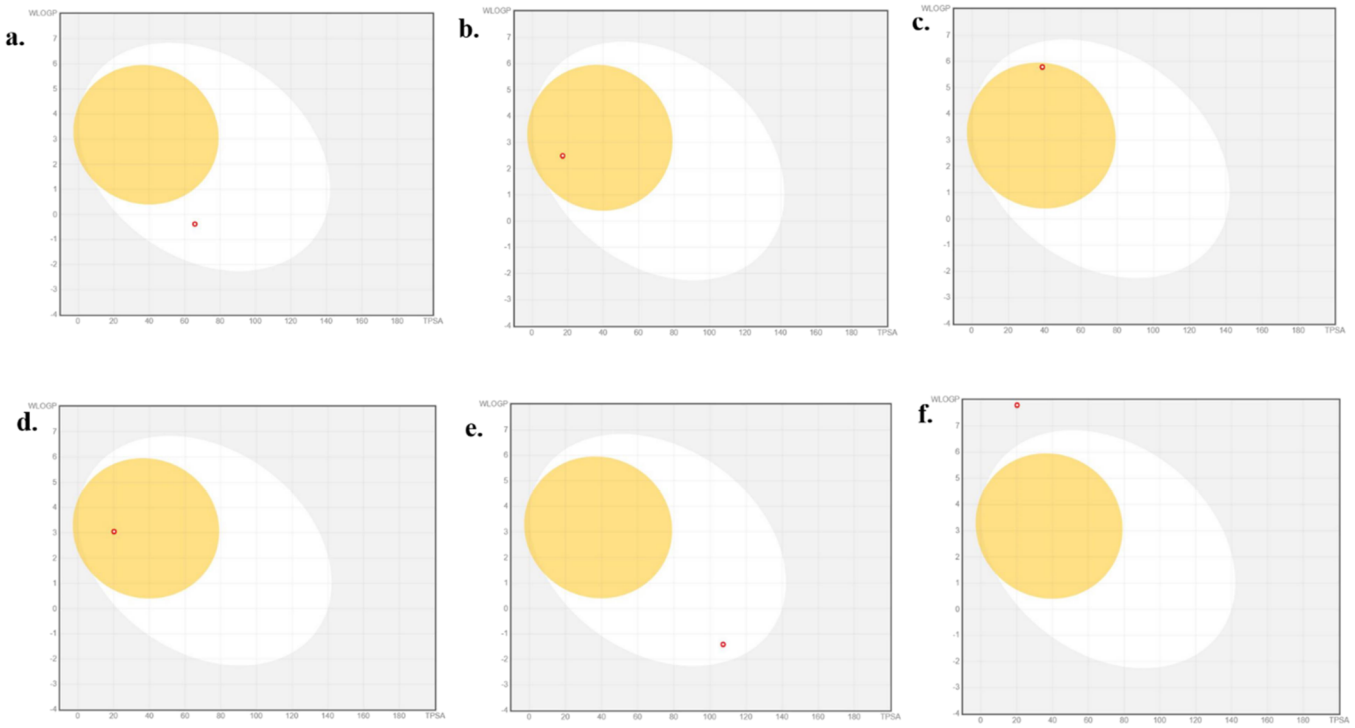

Figure 4. BOILED-Egg Model of compounds (a) 5-fluorouracil, (b) safranal, (c) tigogenin, (d) *trans-p*-mentha-2,8-dienol, (e) ascorbic acid, and (f) stigmasterol.

The blood-brain barrier (BBB) and GI absorption are the main factors in the drug development process. The quantity absorbed by the intestinal system of the drug candidates is one of the major factors in oral bioavailability. Investigating the intestinal absorption of drug candidates is crucial to oral bioavailability. P-Glycoprotein (PGsP) is an ABC transporter and an ATP Binding Cassette family (ABC) member. Functioning as a biological barrier, it removes toxins and xenobiotics from cells and plays an important role in drug absorption and extraction. Overexpression of ABC transporters leads to multidrug resistance (MDR), a crucial factor in the failure of many disease treatments.

The BOILED-egg method predicts GI absorption and BBB penetration of the compounds. This model uses two physicochemical parameters: lipophilicity (WLOGP) and polarity (TPSA). In the Figure. 4, the yellow regions of the BOILED-egg model mean the compound has good permeation and absorption ability in both BBB and GI.[49] If the drug candidate is in the white region of the model, it has good GI absorption but not good BBB penetration. The dots (blue and red) show predictions that the compound can be effluxed and cannot be effluxed from the CNS by PGP, respectively.

We can conclude from the red dots position in our compounds BOILED-Egg models safranal, tigogenin, and *trans-p*-mentha-2,8-dienol show positive BBB penetration, GI absorption property is positive, and the PGP effect on the molecule is negative. 5-FU and ascorbic acid show BBB penetration, PGP effects are negative, and GI absorption properties are positive. However, stigmasterol shows negative BBB, GI absorption, and PGP effects.

3.5. Toxicity Potential of Selected Compounds. We further screened the P5S-derived compounds based on their toxicity potential using Data Warrior. Data Warrior is an open and interactive software for data analysis that incorporates well-established and novel chemoinformatics algorithms in a single environment.[36] All of the selected P5S active compounds had no toxicity, except safranal, which showed irritant behavior (Table 6).

3.6. PaccMann Analysis for the Anticancer Sensitivity Prediction. PaccMann web service (https://ibm.biz/paccmann-aas), is an open-access, web-based platform. This

https://doi.org/10.1021/acsomega.4c07924
ACS Omega 2025, 10, 871−884

Table 6. Toxicity Potential of the Selected Panch Phoron-Derived Compounds Obtained from Data Warrior

	toxicity risks			
compounds name	tumorigenesis	irritant	reproductive effect	mutagenic
5-FU	high	high	high	high
safranal	none	high	none	none
tigogenin	none	none	none	none
trans-p-mentha-2,8-dienol	none	none	none	none
ascorbic acid	none	none	none	none
stigmasterol	none	none	none	none

is a multimodal deep learning model for drug sensitivity prediction that integrates three key pillars of information: first the structure of the compounds as SMILES sequence, second gene expression profiles (GEP) of tumors, and last prior knowledge on intracellular interactions from protein−protein interaction networks to predict drug sensitivity as measured by IC_{50} (half maximal inhibitory concentration) on drug-cell-pairs. So with the help of the PaccMann model, we found that stigmasterol and tigogenin show the lowest IC-50 against cancers (Supplementary Data 2).

Stigmasterol and Tigogenin exhibited the lowest IC_{50} values NCIH3255 (−0.643 and 1.297, respectively); ascorbic acid and *trans-p*-mentha-2,8-dienol showed the lowest IC_{50} in SW1573 (1.802 and 1.298, respectively), while Safranal showed the lowest IC_{50} in LC1F (2.67). Interestingly the origin of all these three cell lines is lung cancer.

3.7. DFT (Density Functional Theory Analysis): To Check the Chemical Stability of Ligands. Density functional theory (DFT) analysis revealed the stability of all of the molecules. The values revealed that tigogenin had the highest chemical electronic energy (−1828.54 Hartree) compared with stigmasterol (−1567.43 Hartree). This approach is based on the capability of a ligand to transport electrons and its chemical stability. Whenever the ligands are bound to the protein, there is a difference between their highest occupied molecular orbitals (HOMO) and lowest unoccupied molecular orbitals (LUMO) (Figure 5).

3.8. Molecular Dynamics Simulation (Complex Stability Study). The top two ligands were used to study the interactions between the protein−ligand complexes. The most stable protein−ligand complexes obtained from molecular docking were further subjected to molecular dynamics simulations to gain a detailed insight into the structural stability and internal movements of the protein−ligand complex over a time scale of 100 ns (Figure 6).

To gain a comprehensive understanding of the complex's stability, the MDS was done. This method is required to gain insight into the correlation between macromolecule structures and function.[50] RMSD denotes the frequency with which deviations are observed during the simulation's evolution. Additionally, the RMSD value indicates the protein's stability; a lower RMSD value corresponds to higher consistency.[51] The stability of stigmasterol and tigogenin with DNMT1 complexes was assessed through the trajectory analysis obtained through protein−ligand complex RMSD, protein backbone (bb), ligand, and radius of gyration (R_g), and RMSF analysis over a time frame of 100 ns (100,000 ps).

In this study, MDS analysis showed a satisfactory stability profile. With a maximum deviation of 1−2.3 Å (0−100 ns), ATG5 had the highest RMS deviation from zero in the ATG5/stigmasterol complex simulation. Subsequently, in the first phase, a 1 Å variation was noted between 1 and 2 Å at a time interval of 0−30 ns. An RMS divergence of 1.5 to 2.25 Å was noted after 30 ns from 30−100 ns time. From 0 to 100 ns, the complex showed stability with deviations of 1−2 Å, whereas small globular proteins could tolerate variations of up to 3 Å.[42] The root-mean-square deviation (RMSD) of the ligand remained steady within the range of 0 to 22 ns, with a deviation ranging from 1.7 to 2.3 Å. The most notable deviations occurred during the first phase, from 22 to 39 ns, with the largest deviation recorded between 2.3 and 4.9 Å. Following that, we had seen a decrease in the ligand's RMS deviation and its stability between 1.19 and 2.4 Å with notable variances. The protein−ligand complex was shown to be stable with minor variations after simulation (Figure 6(i)A).[52,53] The majority of the interacting amino acid RMS variations were observed in the C- and N-termini of the protein (Figure 6 (i)B). The complex interaction fractions revealed that, over 100 ns, less than 10% of the residues Val^{7}, Val^{11}, Ile^{243}, Pro^{245}, Met^{246}, Trp^{253}, Leu^{254}, and Leu^{258} were involved in hydrophobic interactions. On the other hand, Phe^{13}, Arg^{15}, and Arg^{41}

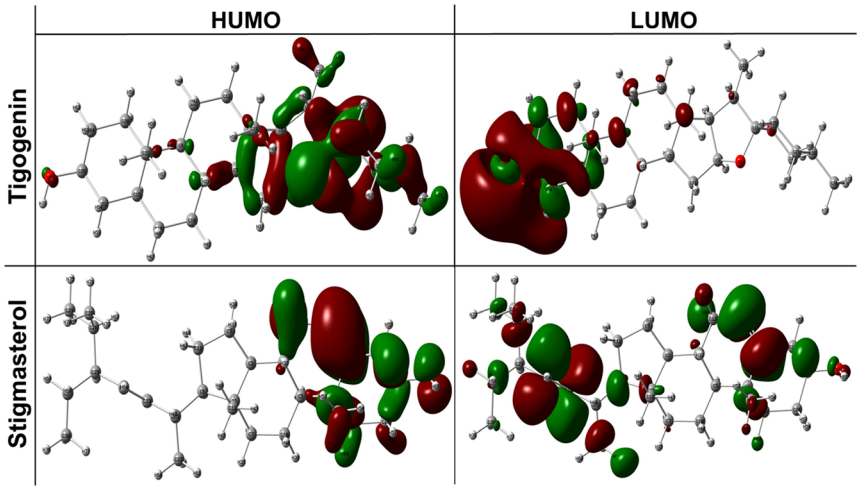

Figure 5. DFT evaluation: Both stigmasterol and tigogenin ligands have different charge distributions in their HOMO and LUMO models. The red color represents negative electron density, whereas the green color represents positive electron density.

https://doi.org/10.1021/acsomega.4c07924
ACS Omega 2025, 10, 871−884

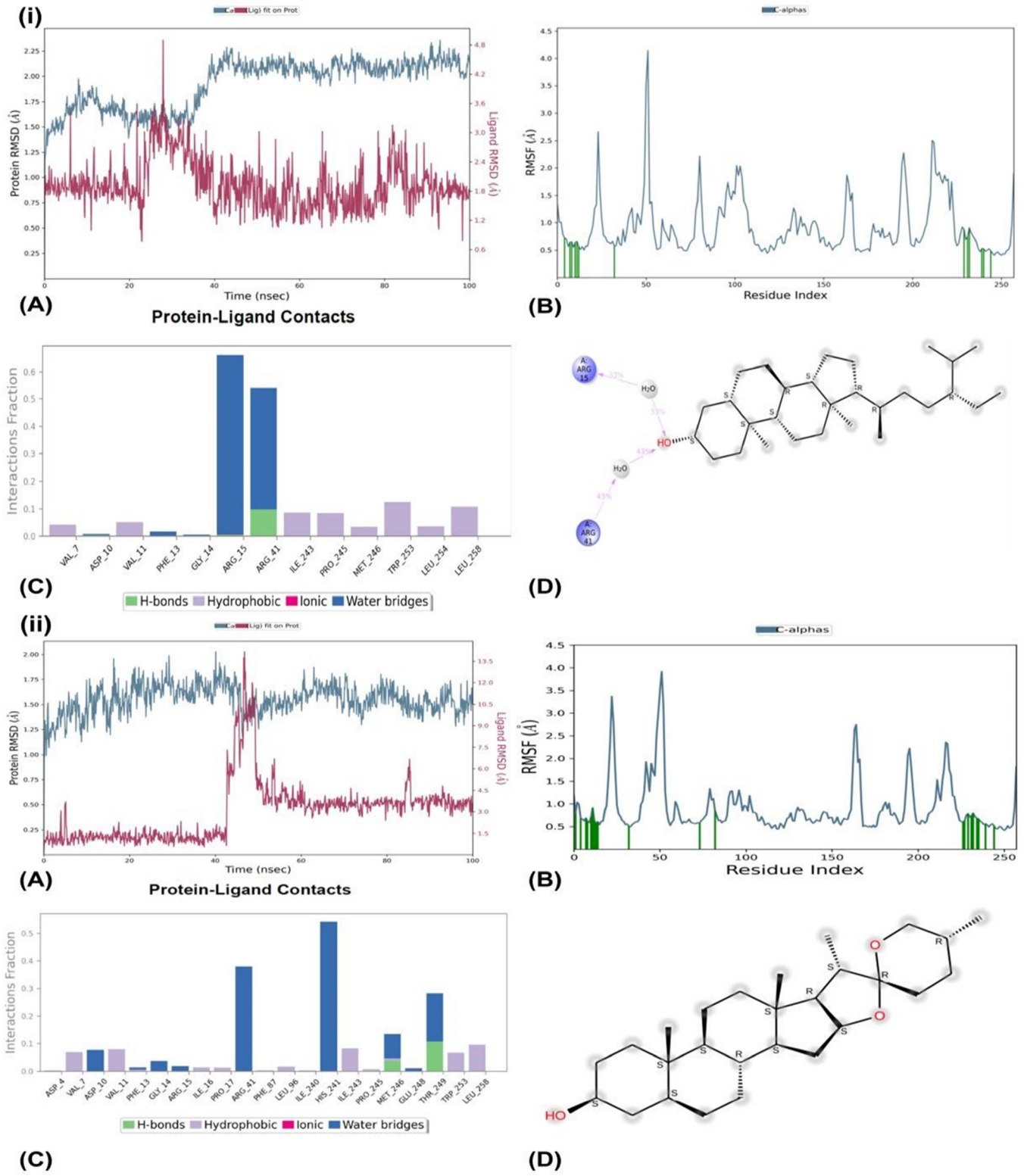

Figure 6. (i) (A) RMSD profile of the ATG5/stigmasterol complex. (B) RMSF profile of ATG5 of the stigmasterol complex. (C) Protein−ligand interaction of the ATG5/stigmasterol complex. (D) Ligand-protein contact profile of ATG5 of the stigmasterol complex. (ii) (A) RMSD profile of the ATG5/tigogenin complex. (B) RMSF profile of the ATG5/tigogenin complex. (C) Protein−ligand interaction of the ATG5/tigogenin complex. (D) Ligand-protein contact profile of ATG5 the tigogenin complex.

were implicated in 5−70% of water bridges throughout the 100 ns time period. Additionally, Arg^{41} participated in hydrogen bonding for 10% of the time in the interaction fractions (Figure 6(i)C). However, at 33 and 43% points of the 100 ns simulations, it was shown that A: Arg^{15} and A: Arg^{41} were implicated in hydrophobic interactions via water molecules at the protein−ligand interface. However, no hydrogen bonds were observed (Figure 6(i)D).

https://doi.org/10.1021/acsomega.4c07924
ACS Omega 2025, 10, 871−884

With a maximum deviation of 1−2 Å at the early stage (0−18 ns), ATG5 showed the highest RMS deviation from zero in the ATG5/tigogenin complex simulation. Subsequently, a 1 Å variation was noted between 1 and 2 Å. In contrast, the root-mean-square deviation (RMSD) of the ligand remained steady from Å to 0−45 ns, with the greatest variation occurring from 1−14 Å during the first phase, which lasted from 45 to 58 ns. Following that, we have seen a decrease in the ligand's RMS deviation and its stability between 2.9 and 4.4 Å with very minor fluctuations. The protein−ligand complex was stable with minor variations after the simulation (Figure 6(ii)A). The majority of the interacting amino acid RMS variations were observed in the C- and N-termini of the protein (Figure 6(ii)B). The complex interaction fractions revealed that during a 100 ns MD simulation, Asp^{4}, Asp^{10}, Arg^{15}, Ile^{16}, Ile^{243}, Trp^{253}, and Leu^{258} were residues engaged in hydrophobic interactions in less than 10% of the contacts. On the other hand, it was found that water bridges engaged Val^{7}, Val^{11}, Phe^{13}, Gly^{14}, Arg^{15}, Pro^{17}, Ile^{240}, Pro^{245}, Glu^{248}, and Thr^{249} for 5−55% contact within 100 ns. Moreover, Pro^{245} and Glu^{248} participated in hydrogen bonding between 5% and 10% of the time in the interaction fractions (Figure 6(ii)C). Nevertheless, it was found that there were no hydrophobic or hydrogen bonding interactions in the protein−ligand interactions (Figure 6(ii)D).

Our results demonstrated that in all P5S, stigmasterol and tigogenin showed good binding energies with both molecular targets as well as the best bioactivity score. Our findings also verified that stigmasterol and tigogenin followed most of the parameters of drug discovery and showed the best potency among the selected compounds.

4. DISCUSSION

Many spices are employed as flavoring agents due to their bioactive compounds, which exhibit potent anti-inflammatory, antioxidant, and anticancer activities.[17,54] Natural compounds derived from spices have demonstrated promising potential as autophagy modulators, particularly in the context of cancer prevention and treatment.[55] Compounds such as curcumin, stigmasterol, diosgenin, and quercetin have been shown to influence autophagic pathways, including JAK/STAT, Ras-Raf signaling pathways, Beclin-1 interactome, and PI3K/Akt/mTOR signaling pathway.[56−59]

Recent research has increasingly focused on identifying phytochemicals from spices that can modulate the autophagy pathway with fewer side effects compared to synthetic compounds.[55,60] Although specific data on autophagy modulation by spice-derived compounds is limited, the growing interest in this area is evident, as researchers investigate their potential to regulate autophagy in cancer cells, which may offer new therapeutic avenues.[60] Therefore, further studies on the tumor-suppressive functions of autophagy are required as modulating this process may enhance cancer treatment strategies. Inhibiting autophagy, which often protects tumor cells, could activate apoptosis and sensitize these cells to therapy, making autophagic cell death a viable therapeutic target.[54]

Thus, we used molecular docking interactions to investigate the effects of P5S-derived active compounds on autophagic and apoptotic markers (ATG5, LC3, and CASPASE-3). We simulated the molecular docking of 224 P5S-derived compounds with autophagic and apoptotic proteins. The lowest energy of the best cluster is considered. One of the best interactions was selected from each P5S containing all target molecules. Compounds with the lowest binding energies and inhibition constants with selected markers, along with hydrogen bonds and interacting amino acids, are presented in Table 1. Stigmasterol and tigogenin show the best interaction with ATG5 −8.63 and −8.26 kcal/mol binding energy and 0.47056 and 0.87837 μM inhibition constant, respectively. Autophagy depends on ATG5 during phagophore production, and ATG12−ATG5 binds ATG16L1 through ATG5. ATG16L1 dimerizes and associates with phagophores, thereby expanding the membrane.[3] Knocking down or knocking out ATG5 can result in downregulation or total inhibition of autophagy, suggesting that ATG5 plays a central role in autophagy.[1] LC3 also plays an important role in autophagosome formation in autophagy,[61] and stigmasterol and tigogenin showed the best interaction among all the compounds with LC3 with −8.35 and −7.90 kcal/mol binding energy and inhibition constants of 0.75183 and 1.62 μM inhibition constant, respectively. Furthermore, we checked the interaction between CASPASE-3 and the selected compounds and found that stigmasterol and tigogenin showed the best interaction (Table 2). We also compared molecular docking results with new calculations carried out with CBDock and DockThor servers and found the same results as Autodock (Supplementary Tables 1 and 2). Therefore, it is possible that stigmasterol and tigogenin modulate the role of ATG5, which in turn may help in the modulation of autophagy.

Drug discovery is a lengthy and resource-intensive process, and undesirable pharmacokinetic properties and toxicity remain hurdles in this process. Therefore, it is important to design lead compounds with good pharmacokinetics and bioavailability to avoid late-stage attrition.[62] Molecular descriptors and drug-likeliness properties of the selected compounds were analyzed using Molinspiration Cheminformatics software based on Lipinski Rules of Five.[63] The Lipinski Rules of Five are called the "Rule of Five" because the border values are 5, 500, 2 × 5, and 5.[47] Molecules that violate more than one of these rules may cause bioavailability problems. Therefore, in our study, no compound showed more than one violation. This indicated that all of the selected compounds showed good physicochemical properties (Table 3). We also calculated % of absorption through TPSA and we found all of the compounds showed good absorption. TPSA is a crucial parameter in drug design and pharmacokinetics, as it influences the ability of a compound to permeate biological membranes. Compounds with a TPSA of less than 140 Å are generally considered to have favorable absorption characteristics.[64] All the selected compounds showed less than 140 Å TPSA. Safranal, *trans-p*-mentha-2,8-dienol, and stigmasterol have shown more than 100% absorption. The calculated TPSA can indicate the potential for enhanced permeability, which may lead to absorption values that exceed 100% under certain conditions, particularly when considering the compound's formulation and delivery method.[65]

Bioactivity scores were also checked using Molinspiration Cheminformatics for different targets, such as G-protein coupled receptor (GPCR) ligands, ion channel modulators, kinase inhibitors, nuclear receptor ligands, protease inhibitors, and enzyme inhibitors.[33] Stigmasterol and tigogenin showed excellent GPCR ligand affinity. GPCR plays a significant role in regulating autophagy. GPCRs can modulate the expression of autophagy-related genes, such as Beclin 2, which is involved in the formation of autophagosomes.[66] GPCRs play a dual role in

https://doi.org/10.1021/acsomega.4c07924
ACS Omega 2025, 10, 871−884

autophagy regulation. They not only activate autophagic pathways but also mediate the degradation of autophagy-related proteins. This complexity highlights the importance of GPCR signaling in cellular homeostasis and suggests their potential as therapeutic targets in diseases involving autophagy dysregulation.[67] This suggests that stigmasterol and tigogenin can influence autophagy through GPCRs.

Our results indicated that stigmasterol has better GPCR ligand modulation properties (nuclear receptor ligand > enzyme inhibitor> GPCR ligand > protease inhibitor > ion channel modulator > kinase inhibitor). Tigogenin also exhibits good GPCR ligand modulation properties (enzyme inhibitor > nuclear receptor ligand > ion channel modulator > GPCR ligand > kinase inhibitor) (Table 4).

Except for stigmasterol and tigogenin, all compounds were considered inactive GPCR ligands with bioactivity scores less than −0.50. 5-FU was predicted to be inactive against all targets (GPCR ligands, ion channel modulators, kinase inhibitors, nuclear receptor ligands, protease inhibitors, and enzyme inhibitor targets) and showed a −0.50 bioactive score. Our findings showed that among the selected compounds, stigmasterol and tigogenin had good bioactivity scores. Bioactivity scoring enables rapid virtual screening of compound libraries to select the most promising candidates for experimental testing, saving time and resources. However, these predictions should be validated through experimental assays to confirm the actual biological activity against GPCRs.[68,69] The identification of stigmasterol and tigogenin as potential active compounds demonstrates how this approach can reveal unexpected leads for further development.

Furthermore, ADMET properties were predicted using the pre-ADMET web server (Table 5). Human intestinal absorption (HIA) of a drug is very important for identifying potential drug candidates. All of the selected compounds showed good absorption in the human intestine, except for ascorbic acid. For blood-brain barrier (BBB) penetration, we checked whether selected compounds can cross the BBB, which is crucial in the pharmaceutical sphere because CNS-active compounds are the only substances that must cross the barrier. This was performed to avoid CNS side effects in the brain. In this study, tigogenin, *trans-p*-mentha-2,8-dienol, and safranal were highly absorbed in the CNS. Tigogenin, *trans-p*-mentha-2,8-dienol, and stigmasterol strongly bind to plasma proteins and exhibit more than 90 values. Caco-2 cells are derived from human colon adenocarcinomas and possess multiple drug transport pathways through the intestinal epithelium. All compounds, except ascorbic acid, showed moderate Caco-2 cell permeability.[70]

Gastrointestinal absorption and brain access are two pharmacokinetic behaviors that are crucial to estimating at various stages of the drug discovery processes. We also checked these properties of selected compounds using the BOILED-Egg model. The *Brain Or IntestinaL EstimateD permeation* method (BOILED-Egg) is proposed as an accurate predictive model that works by computing the lipophilicity and polarity of small molecules. Therefore, in this model, safranal, tigogenin, and trans-p-mentha-2,8-dienol also show positive BBB penetration and GI absorption properties, and the PGP effect on the molecule is negative. Next, we checked the anticancer sensitivity of selected compounds through Pacc-Mann Analysis and found that stigmasterol and tigogenin predict the lowest IC-50 among all. In this in silico predictive screening, we observed that all of the top compounds demonstrated the lowest IC50 values against several lung cancer cell lines (NCI-H3255, SW1573, and LC1F) when compared to a diverse panel of 2020 cell lines representing various cancer types. This extensive in silico screening not only highlights the promising anticancer properties of the identified compounds but also suggests potential pathways for further investigation and development in targeted therapies for lung cancer. Future studies will be essential to validate these in silico predictions through in vitro and in vivo experiments to confirm their therapeutic potential.

In this study, we also performed Density Functional Theory (DFT). DFT plays a crucial role in the design and development of new drugs, particularly in understanding the electronic properties of compounds and their interactions with their biological targets. DFT provides insights into the molecular structure, reactivity, and binding affinities of potential drug candidates, which are essential for optimizing their therapeutic efficacy.[71] One of the primary applications of DFT in drug design is the evaluation of the electronic properties of the compounds. Furthermore, DFT calculations can help elucidate the molecular orbitals and electronic transitions of these compounds, providing a deeper understanding of their mechanisms of action at the molecular level.[72] In our study, we found that tigogenin had the highest chemical electronic energy (−1828.54 Hartree) compared to stigmasterol (−1567.43 Hartree). The highest chemical electronic energy in DFT modeling represents the energy of the HOMO, which is fundamental in determining the electronic properties, reactivity, and potential interactions of a compound. That means tigogenin more readily donates electrons compared to stigmasterol. So maybe tigogenin is significant in various chemical processes, including oxidation−reduction reactions and coordination with metal centers in catalysis.

To further investigate the dynamic mobility and structural stability of the autophagic marker ATG5, ATG5/stigmasterol and ATG5/tigogenin complexes were examined over 100 ns. Using molecular dynamics (MD) simulations, we compared and examined the atomic-level interactions between ATG5/stigmasterol and ATG5/tigogenin as well as variations in their binding mechanisms. A molecular dynamics (MD) study showed that there were minor but important differences between the two complexes. The fraction of interaction plots shows the important relationships and contributions during a 100 ns molecular simulation. Further experimental studies are required to prove the strong affinity of these protein−ligand complexes.

5. CONCLUSIONS

In summary, phytochemicals have been of great interest to researchers in identifying potential anticancer drugs through in silico approaches. Our findings suggest that stigmasterol and tigogenin have better binding potential with ATG5, LC3, and CASPASE-3. These compounds may emerge as potential multitarget drugs against autophagy. They also have favorable drug-likeness ability and good ADMET properties and are suitable for human consumption. The expected outcomes of this study will help in increasing the repertoire of anticancer drugs with better potency so that the problem created by the emergence of resistance to standard anticancer drugs can be reduced. Some studies show that stigmasterol has the potential to modulate autophagy, but the complete mechanism of action is still unexplored, while tigogenin is still unexplored with respect to autophagy modulation. Further studies on these two

https://doi.org/10.1021/acsomega.4c07924
ACS Omega 2025, 10, 871−884

compounds via in vitro and in vivo experiments are required. Thus, the active compounds identified in this study show promise as alternative treatments for cancer patients. This study may also provide a new paradigm for treating cancer by using agents that are part of an individual's regular diet.

■ ASSOCIATED CONTENT

Supporting Information

The Supporting Information is available free of charge at https://pubs.acs.org/doi/10.1021/acsomega.4c07924.

Molecular docking interaction images and molecular docking results through CBDock and DockThor (PDF)

Complete PaccMann analysis (XLSX)

■ AUTHOR INFORMATION

Corresponding Author

Snober S. Mir − *Molecular Cell Biology Laboratory, Integral Centre of Excellence for Interdisciplinary Research (ICEIR-4) and Department of Biosciences, Faculty of Science, Integral University, Lucknow, Uttar Pradesh 226026, India;* orcid.org/0000-0002-1984-0232; Email: smir@iul.ac.in

Authors

Sana Parveen − *Molecular Cell Biology Laboratory, Integral Centre of Excellence for Interdisciplinary Research (ICEIR-4) and Department of Biosciences, Faculty of Science, Integral University, Lucknow, Uttar Pradesh 226026, India*

Shoeb Ikhlas − *Department of Cell Biology, Albert Einstein College of Medicine, New York, New York 10461, United States*

Tabrez Faruqui − *Department of Biosciences, Faculty of Science, Integral University, Lucknow, Uttar Pradesh 226026, India*

Adria Hasan − *Molecular Cell Biology Laboratory, Integral Centre of Excellence for Interdisciplinary Research (ICEIR-4) and Department of Bioengineering, Faculty of Engineering, Integral University, Lucknow, Uttar Pradesh 226026, India*

Aisha Khatoon − *Molecular Cell Biology Laboratory, Integral Centre of Excellence for Interdisciplinary Research (ICEIR-4) and Department of Biosciences, Faculty of Science, Integral University, Lucknow, Uttar Pradesh 226026, India*

Mohd Saeed − *Department of Biology College of Science, University of Hail, Hail 2240, Saudi Arabia*

Ali G. Alkhathami − *Department of Clinical Laboratory Sciences, College of Applied Medical Sciences, King Khalid University, Abha 62521, Saudi Arabia*

Samra Siddiqui − *Department of Health Services Management, College of Public Health and Health Informatics, University of Hail, Hail 2240, Saudi Arabia*

Shahab Uddin − *Department of Biosciences, Faculty of Science, Integral University, Lucknow, Uttar Pradesh 226026, India; Translational Research Institute, Academic Health System, Hamad Medical Corporation, Doha 3050, Qatar;* orcid.org/0000-0003-1886-6710

Complete contact information is available at: https://pubs.acs.org/10.1021/acsomega.4c07924

Notes

The authors declare no competing financial interest.

■ ACKNOWLEDGMENTS

We would like to thank the Hon'ble Vice-Chancellor, Integral University, Lucknow for the necessary infrastructure support and the Dean Office, R&D, Integral University for providing the manuscript communication number (IU/R&D/2021-MCN0001230). The authors also express their gratitude to the Deanship of Scientific Research at King Khalid University for funding this work through the Large Research Group Project under grant number RGP.02/534/44.

■ REFERENCES

(1) Li, X.; He, S.; Ma, B. Autophagy and autophagy-related proteins in cancer. *Molecular cancer* **2020**, *19* (1), 1−16.

(2) White, E. The role for autophagy in cancer. *J. Clin. Invest.* **2015**, *125* (1), 42−46.

(3) Patra, S.; Mishra, S. R.; Behera, B. P.; Mahapatra, K. K.; Panigrahi, D. P.; Bhol, C. S.; Praharaj, P. P.; Sethi, G.; Patra, S. K.; Bhutia, S. K. Autophagy-modulating phytochemicals in cancer therapeutics: Current evidences and future perspectives. In *Seminars in Cancer Biology*; Academic Press, 2022, vol *80*, pp 205−217.

(4) Kondo, Y.; Kanzawa, T.; Sawaya, R.; Kondo, S. The role of autophagy in cancer development and response to therapy. *Nature reviews. Cancer* **2005**, *5* (9), 726−734.

(5) Sun, Y.; Peng, Z. L. Programmed cell death and cancer. *Postgraduate medical journal* **2009**, *85* (1001), 134−140.

(6) Onorati, A. V.; Dyczynski, M.; Ojha, R.; Amaravadi, R. K. Targeting autophagy in cancer. *Cancer* **2018**, *124* (16), 3307−3318.

(7) Madia, F.; Worth, A.; Whelan, M.; Corvi, R. Carcinogenicity assessment: Addressing the challenges of cancer and chemicals in the environment. *Environ. Int.* **2019**, *128*, 417−429.

(8) Hasan, A.; Khamjan, N.; Lohani, M.; Mir, S. S. Targeted Inhibition of Hsp90 in Combination with Metformin Modulates Programmed Cell Death Pathways in A549 Lung Cancer Cells. *Appl. Biochem. Biotechnol.* **2023**, *195*, 7338−7378.

(9) Vasanthi, H. R.; Parameswari, R. P. Indian spices for healthy heart - an overview. *Curr. Cardiol. Rev.* **2010**, *6* (4), 274−279.

(10) Peter, K. V.; Shylaja, M. R. Introduction to herbs and spices: definitions, trade and applications. In *Handbook of herbs and spices*; Woodhead Publishing, 2012; pp 1−24.

(11) Kunnumakkara, A. B.; Koca, C.; Dey, S.; Gehlot, P.; Yodkeeree, S.; Danda, D.; Sung, B.; Aggarwal, B. B. Traditional uses of spices: an overview. *Molecular targets and therapeutic uses of spices: modern uses for ancient medicine* **2009**, 1−24.

(12) Gias, Z. T.; Afsana, F.; Debnath, P.; Alam, M. S.; Ena, T. N.; Hossain, M. H.; Jain, P.; Reza, H. M. A mechanistic approach to HPLC analysis, antinociceptive, anti-inflammatory and postoperative analgesic activities of panch phoron in mice. *BMC complementary medicine and therapies* **2020**, *20* (1), 1−9.

(13) Sarkar, D. A Review of the Seeds Comprising Panch phoron, a Spice used in Indian Cuisine. *Int. J. Pharm. Investigation* **2019**, *9* (2), 25−35.

(14) Chamikara, M. D. M.; Dissanayake, D. R. R. P.; Ishan, M.; Sooriyapathirana, S. D. S. S. Dietary, anticancer and medicinal properties of the phytochemicals in chili pepper (Capsicum spp.). *Ceylon J. Sci.* **2016**, *45* (3), 5−20.

(15) Aggarwal, B. B.; Kunnumakkara, A. B.; Harikumar, K. B.; Tharakan, S. T.; Sung, B.; Anand, P. Potential of spice-derived phytochemicals for cancer prevention. *Planta medica* **2008**, *74* (13), 1560−1569.

(16) Basu, S.; Banik, B. K. Natural spices in medicinal chemistry: Properties and benefits. In *Green Approaches in Medicinal Chemistry for Sustainable Drug Design*; Elsevier, 2020; pp 739−758.

(17) Kammath, A. J.; Nair, B.; P, S.; Nath, L. R. Curry versus cancer: Potential of some selected culinary spices against cancer with in vitro, in vivo, and human trials evidences. *Journal of Food Biochemistry* **2021**, *45* (3), No. e13285.

(18) El-Shafey, E. S.; Elsherbiny, E. S. Dual opposed survival-supporting and death-promoting roles of autophagy in cancer cells: a concise review. *Current Chemical Biology* **2020**, *14* (1), 4−13.
(19) Huang, R.; Liu, W. Identifying an essential role of nuclear LC3 for autophagy. *Autophagy* **2015**, *11* (5), 852−853.
(20) Wang, J.; Sun, S.; Liu, L.; Yang, W. Induction of apoptosis in human cervical carcinoma hela cells with active components of menispermum dauricum. *Genetics and Molecular Research* **2014**, *13* (2), 3545−3552.
(21) Wang, Y.; Liu, C.; Wang, J.; Zhang, Y.; Chen, L. Iodine-131 induces apoptosis in human cardiac muscle cells through the p53/bax/caspase-3 and pidd/caspase-2/t-bid/cytochrome c/caspase-3 signaling pathway. *Oncol. Rep.* **2017**, *38* (3), 1579−1586.
(22) Zhu, Y.; Zhao, L.; Liu, L.; Gao, P.; Tian, W.; Wang, X.; Chen, Q. Beclin 1 cleavage by caspase-3 inactivates autophagy and promotes apoptosis. *Protein Cell* **2010**, *1* (5), 468−477.
(23) Kasikci, M.; Sen, S. Resveratrol and quercetin protect from benzo(a)pyrene-induced autophagy in retinal pigment epithelial cells. *Int. Ophthalmol.* **2024**, *44* (1), 12.
(24) Ma, D.; Huang, Y.; Song, S. Inhibiting the HPV16 oncogene-mediated glycolysis sensitizes human cervical carcinoma cells to 5-fluorouracil. *Onco Targets Ther.* **2019**, 6711−6720.
(25) Huang, J.; Wu, Z.; Xu, J. Effects of biofilm nano-composite drugs omvs-msn-5-fu on cervical lymph node metastases from oral squamous cell carcinoma. *Front. Oncol.* **2022**, *12*, No. 881910.
(26) Pan, X.; Zhang, X.; Sun, H.; Zhang, J.; Yan, M.; Zhang, H. Autophagy inhibition promotes 5-fluorouraci-induced apoptosis by stimulating ros formation in human non-small cell lung cancer a549 cells. *PLoS One* **2013**, *8* (2), No. e56679.
(27) Li, Z.; Wan, H.; Shi, Y.; Ouyang, P. Personal experience with four kinds of chemical structure drawing software: review on ChemDraw, ChemWindow, ISIS/Draw, and ChemSketch. *Journal of chemical information and computer sciences* **2004**, *44* (5), 1886−1890.
(28) Berman, H. M.; Westbrook, J.; Feng, Z.; Gilliland, G.; Bhat, T. N.; Weissig, H.; Shindyalov, I. N.; Bourne, P. E. The protein data bank. *Nucleic acids research* **2000**, *28* (1), 235−242.
(29) Prada-Gracia, D.; Huerta-Yépez, S.; Moreno-Vargas, L. M. Application of computational methods for anticancer drug discovery, design, and optimization. *Bol. Med. Hosp. Infant Mex.* **2016**, *73* (6), 411−423.
(30) Rizvi, S. M. D.; Shakil, S.; Haneef, M. A simple click by click protocol to perform docking: AutoDock 4.2 made easy for non-bioinformaticians. *EXCLI J.* **2013**, *12*, 831−857.
(31) Liu, Y.; Grimm, M.; Dai, W. T.; Hou, M. C.; Xiao, Z. X.; Cao, Y. CB-Dock: A web server for cavity detection-guided protein−ligand blind docking. *Acta Pharmacologica Sinica* **2020**, *41* (1), 138−144.
(32) Guedes, I. A.; Krempser, E.; Dardenne, L. E. DockThor 2.0: a free web server for protein-ligand virtual screening. *XIX SBQT−Simpósio Brasileiro de Química Teórica*, 2017, vol *2013*; pp 2013−2014.
(33) Bhat, A. R. Petra, osiris and molinspiration: A computational bioinformatic platform for experimental in vitro antibacterial activity of annulated uracil derivatives. *Iranian Chem. Commun.* **2018**, *6* (2), 114−124.
(34) Jaitak, V. Molecular docking study of natural alkaloids as multi-targeted hedgehog pathway inhibitors in cancer stem cell therapy. *Comput. Biol. Chem.* **2016**, *62*, 145−154.
(35) Rashid, M. Design, synthesis and ADMET prediction of bis-benzimidazole as anticancer agent. *Bioorganic chemistry* **2020**, *96*, No. 103576.
(36) López-López, E.; Naveja, J. J.; Medina-Franco, J. L. DataWarrior: An evaluation of the open-source drug discovery tool. *Expert Opinion on Drug Discovery* **2019**, *14* (4), 335−341.
(37) Sripriya, N.; Ranjith Kumar, M.; Ashwin Karthick, N.; Bhuvaneswari, S.; Udaya Prakash, N. K. *In silico* evaluation of multispecies toxicity of natural compounds. *Drug Chem. Toxicol.* **2019**, *44* (5), 480−486.
(38) Cadow, J.; Born, J.; Manica, M.; Oskooei, A.; Rodríguez Martínez, M. PaccMann: a web service for interpretable anticancer compound sensitivity prediction. *Nucleic acids research* **2020**, *48* (W1), W502−W508.
(39) Kumer, A.; Sarker, M. N.; Sunanda, P. The theoretical investigation of HOMO, LUMO, thermophysical properties and QSAR study of some aromatic carboxylic acids using HyperChem programming. *Int. J. Chem. Technol.* **2019**, *3* (1), 26−37.
(40) Becke, A. D. Density-functional thermochemistry. I. The effect of the exchange-only gradient correction. *J. Chem. Phys.* **1992**, *96* (3), 2155−2160.
(41) Becke, A. D. A new mixing of Hartree−Fock and local density-functional theories. *J. Chem. Phys.* **1993**, *98* (2), 1372−1377.
(42) Bowers, K. J.; Chow, E.; Xu, H.; Dror, R. O.; Eastwood, M. P.; Gregersen, B. A.; Klepeis, J. L.; Kolossvary, I.; Moraes, M. A.; Sacerdoti, F. D.; Salmon, J. K. Scalable algorithms for molecular dynamics simulations on commodity clusters. In *Proceedings of the 2006 ACM/IEEE Conference on Supercomputing*, 2006; pp 84-es.
(43) Sastry, G. M.; Adzhigirey, M.; Day, T.; Annabhimoju, R.; Sherman, W. Protein and ligand preparation: parameters, protocols, and influence on virtual screening enrichments. *J. Computer-Aided Mol. Des.* **2013**, *27* (3), 221−234.
(44) Shivakumar, D.; Williams, J.; Wu, Y.; Damm, W.; Shelley, J.; Sherman, W. Prediction of absolute solvation free energies using molecular dynamics free energy perturbation and the OPLS force field. *J. Chem. Theory Comput.* **2010**, *6* (5), 1509−1519.
(45) Benet, L. Z.; Hosey, C. M.; Ursu, O.; Oprea, T. I. BDDCS, the Rule of 5 and drugability. *Advanced drug delivery reviews* **2016**, *101*, 89−98.
(46) Namachivayam, B.; Raj, J. S.; Kandakatla, N. 2D, 3D-QSAR, docking and optimization of 5-substituted-1H-Indazole as inhibitors of GSK3β. *Int. J. Pharm. Pharm. Sci.* **2014**, *6* (10), 413−420.
(47) Lipinski, C. A.; Lombardo, F.; Dominy, B. W.; Feeney, P. J. Experimental and computational approaches to estimate solubility and permeability in drug discovery and development settings. *Advanced drug delivery reviews* **2001**, *46* (1−3), 3−26.
(48) Jamuna, S.; Rathinavel, A.; Sadullah, S. S. M.; Devaraj, S. N. In silico approach to study the metabolism and biological activities of oligomeric proanthocyanidin complexes. *Indian J. Pharmacol.* **2018**, *50* (5), 242−250.
(49) Şahin, S.; Dege, N. Synthesis, characterization, X-ray, HOMO-LUMO, MEP, FT-IR, NLO, Hirshfeld surface, ADMET, boiled-egg model properties and molecular docking studies with human cyclophilin D (CypD) of a Schiff base compound:(E)-1-(5-nitro-2-(piperidin-1-yl) phenyl)-N-(3-nitrophenyl) methanimine. *Polyhedron* **2021**, *205*, No. 115320.
(50) Hospital, A.; Goñi, J. R.; Orozco, M.; Gelpí, J. L. Molecular dynamics simulations: advances and applications. *Adv. Appl. Bioinform. Chem.* **2015**, *8*, 37−47.
(51) Aier, I.; Varadwaj, P. K.; Raj, U. Structural insights into conformational stability of both wild-type and mutant EZH2 receptor. *Sci. Rep.* **2016**, *6*, 34984.
(52) Faruqui, T.; Singh, G.; Khan, S.; Khan, M. S.; Akhter, Y. Differential gene expression analysis of RAGE-S100A6 complex for target selection and the design of novel inhibitors for anticancer drug discovery. *Journal of cellular biochemistry* **2023**, *124* (2), 205−220.
(53) Kumar, P.; Faruqui, T.; Yadav, A. K.; Chandra, D.; Verma, S.; Saha, S.; Jat, J. L.; Akhter, Y. Targeting caspase pathway by novel N-Me aziridine derivatives for hepatocellular carcinoma drug discovery. *J. Biomol. Struct. Dyn.* **2023**, *42*, 12981−12992.
(54) Wang, N.; Feng, Y. Elaborating the role of natural products-induced autophagy in cancer treatment: achievements and artifacts in the state of the art. *BioMed Res. Int.* **2015**, *2015*, No. 934207.
(55) Rhim, H.; Rhim, H.; Rhim, H.; Uddin, M. J.; Biswas, P.; Islam, R.; Hossain, M. S.; Rahman, M. H.; Rahman, M. A.; Rahman, M. A.; Rahman, M. H.; Rahman, M. A.; Rahman, M. H. Molecular Insights into the Multifunctional Role of Natural Compounds: Autophagy Modulation and Cancer Prevention. *Biomedicines* **2020**, *8* (11), 517.
(56) Zhang, X.; Chen, L.-X.; Ouyang, L.; Cheng, Y.; Liu, B. Plant natural compounds: targeting pathways of autophagy as anti-cancer therapeutic agents. *Cell Proliferation* **2012**, *45* (5), 466−476.

https://doi.org/10.1021/acsomega.4c07924
ACS Omega 2025, 10, 871−884

(57) Bakrim, S.; Sheikh, R. A.; Goh, K. W.; Bouyahya, A.; Benkhaira, N.; Bourais, I.; El Omari, N.; Benali, T.; Ming, L. C.; Lee, L.-H. Health Benefits and Pharmacological Properties of Stigmasterol. *Antioxidants* **2022**, *11* (10), 1912.
(58) Ren, Q.-L.; Yang, X.-T.; Liu, J.-G.; Hu, H.; Ran, Y.-H.; Zhang, X.-Q.; Wang, Q.; Liu, H.-H.; Wang, M.; Tang, J.-J.; Song, Z.-X.; Li, X.-L. Anticancer Activity of Diosgenin and Its Molecular Mechanism. *Chinese Journal of Integrative Medicine* **2023**, *29* (8), 738−749.
(59) Jiang, S.; Fan, J.; Wang, Q.; et al. Diosgenin induces ROS-dependent autophagy and cytotoxicity via mTOR signaling pathway in chronic myeloid leukemia cells. *Phytomedicine.* **2016**, *23*, 243−252.
(60) Moosavi, M. A.; Haghi, A.; Rahmati, M.; Taniguchi, H.; Mocan, A.; Echeverría, J.; Gupta, V. K.; Tzvetkov, N. T.; Atanasov, A. G. Phytochemicals as potent modulators of autophagy for cancer therapy. *Cancer Letters* **2018**, *424*, 46−69.
(61) Nishimura, T.; Tooze, S. A. Emerging roles of ATG proteins and membrane lipids in autophagosome formation. *Cell discovery* **2020**, *6* (1), 32.
(62) Adegbola, P. I.; Semire, B.; Fadahunsi, O. S.; Adegoke, A. E. Molecular docking and ADMET studies of Allium cepa, Azadirachta indica and Xylopia aethiopica isolates as potential anti-viral drugs for Covid-19. *VirusDisease* **2021**, *32* (1), 85−97.
(63) Sander, T.; Freyss, J.; von Korff, M.; Rufener, C. DataWarrior: an open-source program for chemistry aware data visualization and analysis. *J. Chem. Inf. Model.* **2015**, *55* (2), 460−473.
(64) Paramashivam, S. K.; Elayaperumal, K.; Natarajan, B. B.; Ramamoorthy, M. D.; Balasubramanian, S.; Dhiraviam, K. N. In silico pharmacokinetic and molecular docking studies of small molecules derived from Indigofera aspalathoides Vahl targeting receptor tyrosine kinases. *Bioinformation* **2015**, *11* (2), 73−84.
(65) Burayag, L. Predicted inflammatory protein targets of tinospora cordifolia secondary metabolites: admet and molecular docking studies. *Acta Manil.* **2024**, *72*, 33−54.
(66) He, C.; Wei, Y.; Sun, K.; Li, B.; Dong, X.; Zou, Z.; et al. Beclin 2 functions in autophagy, degradation of g protein-coupled receptors, and metabolism. *Cell* **2013**, *154* (5), 1085−1099.
(67) Zhang, T.; Dong, K.; Liang, W.; Xu, D.; Xia, H.; Geng, J.; Yuan, J. G-protein-coupled receptors regulate autophagy by zbtb16-mediated ubiquitination and proteasomal degradation of atg14l. *Elife* **2015**, *4*, No. e06734.
(68) Li, Y.; Wang, R.; Hu, L. A.; Zhong, W.; Sun, Y.; Li, X.; Ma, Y.; Song, Y.; Zhao, Z.; Dai, D.; Zhang, Q. Fragment-Based Computational Method for Designing GPCR Ligands. *J. Chem. Inf. Model.* **2020**, *60* (9), 4339−4349.
(69) Navratilova, I.; Hopkins, A. L.; Besnard, J. Screening for GPCR Ligands Using Surface Plasmon Resonance. *ACS Med. Chem. Lett.* **2011**, *2* (7), 549−554.
(70) Pratama, M. R. F.; Poerwono, H.; Siswodiharjo, S. ADMET properties of novel 5-O-benzoylpinostrobin derivatives. *Journal of Basic and Clinical Physiology and Pharmacology* **2019**, *30* (6), 20190251.
(71) Tandon, H.; Chakraborty, T.; Suhag, V. A brief review on importance of DFT in drug design. *Res. Med. Eng. Sci.* **2019**, *7* (4), 791−795.
(72) Abdelrheem, D. A.; Rahman, A. A.; Elsayed, K. N.; Abd El-Mageed, H. R.; Mohamed, H. S.; Ahmed, S. A. Isolation, characterization, in vitro anticancer activity, dft calculations, molecular docking, bioactivity score, drug-likeness and admet studies of eight phytoconstituents from brown alga sargassum platycarpum. *Journal of molecular structure* **2021**, *1225*, No. 129245.

https://doi.org/10.1021/acsomega.4c07924
ACS Omega 2025, 10, 871−884